



Original article

Flavonoids from the stems of *Millettia pachyloba* Drake mediate cytotoxic activity through apoptosis and autophagy in cancer cells



Wei Yan^{a,1}, Jianhong Yang^{a,1}, Huan Tang^a, Linlin Xue^a, Kai Chen^b, Lun Wang^b, Min Zhao^a, Minghai Tang^a, Aihua Peng^a, Chaofeng Long^c, Xiaoxin Chen^c, Haoyu Ye^{a,*}, Lijuan Chen^a

^a Lab of Natural Product Drugs and Cancer Biotherapy, West China Hospital, West China Medical School, Sichuan University, Chengdu 610041, People's Republic of China

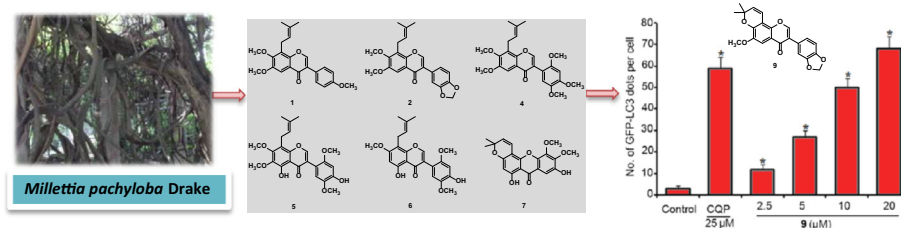
^b School of Chemical Engineering, Sichuan University, Chengdu 610041, People's Republic of China

^c Guangdong Zhongsheng Pharmaceutical Co Ltd., Dongguan 440100, People's Republic of China

HIGHLIGHTS

- Six new natural compounds were isolated from *Millettia pachyloba* Drake.
- The cytotoxic activities of these new compounds were evaluated.
- Ten (3–5, 9, 12, 17–19, 24, and 25) of 28 isolated compounds showed cytotoxicity.
- The ten cytotoxic compounds induced autophagy in cancer cells.
- Compound 9 induced apoptosis and autophagy, suggesting it could be a potential anticancer drug candidate.

GRAPHICAL ABSTRACT



ARTICLE INFO

Article history:

Received 26 April 2019

Revised 18 June 2019

Accepted 18 June 2019

Available online 21 June 2019

Keywords:

Millettia pachyloba

Leguminosae

Isoflavones

Cytotoxicity

Autophagy

Apoptosis

ABSTRACT

In this study, systematic separation and subsequent pharmacological activity studies were carried out to identify cytotoxic natural products from the dried stems of *Millettia pachyloba* Drake. Five previously undescribed isoflavones, pachyvenes A–E; one previously undescribed xanthone, pachythone A; and twenty-two known compounds were obtained. The structures of these compounds were assigned on the basis of 1D/2D NMR data and high-resolution electrospray ionization mass spectroscopy analysis. Preliminary activity screening with HeLa and MCF-7 cells showed that ten compounds (3–5, 9, 12, 17–19, 24, and 25) had potential cytotoxicity. Further in-depth activity studies with five cancer cell lines (HeLa, HepG2, MCF-7, Hct116, and MDA-MB-231) and one normal cell line (HUVEC) revealed that these ten compounds showed specific cytotoxicity in cancer cells, with IC₅₀ values ranging from 5 to 40 μM, while they had no effect on normal cell lines. To investigate whether the cytotoxicity of these ten compounds was associated with autophagy, their autophagic effects were evaluated in GFP-LC3-HeLa cells. The results demonstrated that compound 9 (durmillone) significantly induced autophagy in a concentration-dependent manner and had the best activity as an autophagy inducer among all of the compounds. Therefore, compound 9 was selected for further study. The PI/Annexin V double staining assay and Western blotting results revealed that compound 9 also induced obvious apoptosis in HeLa and MCF-7 cells, which suggests that it mediates cytotoxic activity through activation of both apoptosis and autophagy. Taken together, this study identified ten natural cytotoxic products from the dried stems

Peer review under responsibility of Cairo University.

* Corresponding author.

E-mail address: haoyu_ye@scu.edu.cn (H. Ye).

¹ These authors equally contributed to this paper.

<https://doi.org/10.1016/j.jare.2019.06.002>

2090-1232/© 2019 The Authors. Published by Elsevier B.V. on behalf of Cairo University.

This is an open access article under the CC BY-NC-ND license (<http://creativecommons.org/licenses/by-nc-nd/4.0/>).

of *Millettia pachyloba* Drake, of which compound **9** induced apoptosis and autophagy and could be an anticancer drug candidate.

© 2019 The Authors. Published by Elsevier B.V. on behalf of Cairo University. This is an open access article under the CC BY-NC-ND license (<http://creativecommons.org/licenses/by-nc-nd/4.0/>).

Introduction

Millettia (Leguminosae) is a genus with approximately 200 species that are primarily distributed in tropical and subtropical regions, such as Africa, Asia, America, and Australia [1]. Historically, *Millettia* is a traditional medicine used in the treatment of gynecological diseases, dysentery, cardiovascular diseases, intestinal pain, rheumatic arthritis, and skin diseases [2,3]. Previous phytochemical investigations of this genus have demonstrated the presence of steroids, alkaloids, triterpenoids, and flavonoids [4–7].

Millettia pachyloba Drake (*M. pachyloba*) belongs to the Leguminosae family and is a type of semi-evergreen perennial woody vine plant primarily distributed in the Guangdong, Hainan, Guangxi, and Yunnan Provinces of China. The stems of *M. pachyloba* are often used by locals as a herbal medicine for the treatment of tumors, rheumatic arthritis and removing edema from patients. To date, only three studies have focused on the phytochemical study of *M. pachyloba* [8–10], which is far from providing a deep understanding of *M. pachyloba*. Thus, further intensive phytochemical study of *M. pachyloba* is needed.

Autophagy is the primary cellular process for protecting cells and organisms from natural stressors such as ER-stress as well as nutrient deficiency. In addition to its function in normal physiology, autophagy also plays a role in cancer [11]. Recently, it was established as a tumor suppression mechanism; loss of autophagy function was required for the initiation of cancer [12]. Because previous research reported that isolated flavonoids from *M. pachyloba* exhibited initial cytotoxicity against KB cells [8], it was worthwhile screening the autophagy inducer in *M. pachyloba* and further testing the underlying mechanism. Durmillone is an isoflavone with a dimethyl pyran moiety connected to C6 and C7. It is widespread in the genus of *Millettia* [13,14] and *Lonchocarpus* [15]. However, there is no research reporting its cytotoxic mechanism of action.

This study carried out intensive phytochemical study of *M. pachyloba*. In addition, the initial cytotoxic mechanism of action of the compounds separated from *M. pachyloba* were investigated.

Material and methods

General experimental procedures

The following equipment and methods were used in the present study: silica gel column chromatography (200–300 mesh, Qingdao Makall Group Co., Qingdao, China), Sephadex LH-20 column chromatography (GE Healthcare Bio-Sciences AB, Uppsala, Sweden), high-performance liquid chromatography (HPLC, Waters, Milford, USA), a Sunfire C₁₈ column (5 μm, 4.6 mm × 150 mm; Waters, Milford, USA), a semipreparative HPLC instrument (SP-HPLC, NovaSep, Miramas, France), a digital polarimeter for optical rotation measurements (Jasco P-1020, Tokyo, Japan), a UV-2100 spectrophotometer for ultraviolet absorbance detection (Shimadzu, Kyoto, Japan), a Nicolet-6700 FT-IR spectrometer for IR spectral detection (Thermo Scientific, Waltham, USA), an Aviv Model 400 CD spectrometer (Aviv Biomedical, Lakewood, USA), an Avance-400 spectrometer for NMR spectral detection (Bruker, Billerica, USA), and a Q-TOF Premier mass spectrometer coupled with an ESI source (Waters, Milford, USA).

Plant material

Researcher Hua Peng (Kunming Institute of Botany, Chinese Academy of Sciences) collected and identified the stems of *M. pachyloba* at Pingbian, Yunan, China, in September 2015. A voucher specimen (SKLB-201509) was deposited in the Lab of Natural Product Drugs and Cancer Biotherapy, Sichuan University.

Extraction and isolation

Air-dried stems of *M. pachyloba* (10 kg) were ground into powder (approximately 20-mesh). The powder was extracted with 60 L 95% aqueous EtOH three times. The EtOH extracts were combined and evaporated to dryness *in vacuo* to produce 712 g crude sample. It was then suspended in 5 L deionized H₂O and successively exhausted with 5 L petroleum ether and 5 L CH₂Cl₂ to give dried petroleum ether (48 g) and CH₂Cl₂ (77 g) extracts, respectively, for further separation.

The petroleum ether extract was subjected to silica gel column chromatography (petroleum ether/EtOAc from 100/1 to 1/1, v/v) for rough separation, and eleven fractions (Fr. A1–Fr. A11) were collected. Fr. A5 (1.3 g) was subjected to SP-HPLC (MeOH/H₂O, 75/25, v/v) to yield 7.8 mg of compound **18**. Fr. A7 (1.7 g) was also subjected to SP-HPLC (MeOH/H₂O, 85/15, v/v) to yield 15.7 mg of compound **1**. Fr. A8 (3.9 g) was subjected to silica gel column chromatography (petroleum ether/EtOAc from 20/1 to 1/5, v/v) and produced five subfractions (Fr. A8.1–Fr. A8.5). Fr. A8.2 was subjected to SP-HPLC (MeOH/H₂O, 80/20, v/v) to produce 135.5 mg compound **6**, 5.1 mg compound **7**, and 15.4 mg compound **9**. Fr. A8.3 was subjected to Sephadex LH-20 column chromatography (CH₂Cl₂/MeOH from 10/1 to 1/5, v/v) to yield 83.4 mg compound **22** and 112.7 mg compound **23**. Fr. A9 (2.8 g) was subjected to silica gel column chromatography (petroleum ether/EtOAc, from 20/1 to 1/5, v/v) and further purified by SP-HPLC (MeOH/H₂O, 80/20 and 85/15, v/v, respectively) to yield 8.7 mg compound **3** and 19.6 mg compound **5**.

The CH₂Cl₂ extract was subjected to silica gel column chromatography (petroleum ether/EtOAc, from 50/1 to 1/5, v/v), and 15 fractions (Fr. B1–Fr. B15) were produced. Fr. B3 (1.3 g) was subjected to SP-HPLC (MeOH/H₂O, 85/15, v/v) to yield 5.9 mg compound **19**. Fr. B5 (4.6 g) was subjected to silica gel column chromatography using petroleum ether/EtOAc (from 20/1 to 1/5, v/v), and six subfractions were obtained (Fr. B5.1–Fr. B5.6). Fr. B5.3 and Fr. B5.5 were subjected to SP-HPLC (MeOH/H₂O, 85/15, and 70/30, respectively) to produce 12.5 mg compound **2** and 16.3 mg compound **25**. Fr. B6 (1.7 g) was purified using SP-HPLC (MeOH/H₂O, 65/35, v/v) to obtain 61.4 mg compound **20**. Fr. B7 (4.8 g) was subjected to silica gel column chromatography (petroleum ether/EtOAc from 20/1 to 1/5, v/v) and further purified using Sephadex LH-20 column chromatography (CH₂Cl₂/MeOH, from 10/1 to 1/5, v/v) to produce 9.3 mg compound **8**, 23.1 mg compound **13** and 17.2 mg compound **21**. Fr. B8 (2.4 g) was subjected to SP-HPLC (MeOH/H₂O, 75/25, v/v) to yield 7.1 mg compound **10**. Fr. B9 (3.6 g) was also subjected to SP-HPLC (MeOH/H₂O, 80/20, and 75/25, respectively) to yield 38.5 mg compound **4** and 21.5 mg compound **11**. Fr. B10 (4.1 g) was separated on a silica gel column (petroleum ether/EtOAc, from 20/1 to 1/5, v/v) and by SP-HPLC (MeOH/H₂O, 75/25, and 65/35, respectively) to yield

47.8 mg compound **12** and 13.7 mg compound **15**. Fr. B11 (4.5 g) was purified in the same manner as Fr. B10 to produce 10.2 mg compound **14**, 36.3 mg compound **24** and 38.1 mg compound **27**. Fr. B12 (2.3 g) underwent Sephadex LH-20 column chromatography (CH₂Cl₂/MeOH, from 10/1 to 1/5, v/v) to yield 18.5 mg compound **16** and 16.1 mg compound **17**. Fr. B13 (3.7 g) underwent Sephadex LH-20 column chromatography (H₂O/MeOH, from 10/1 to 1/5, v/v) to yield 48.3 mg compound **26** and 53.9 mg compound **28**. In total, 28 compounds with purities >98% analyzed by HPLC (Waters, Milford, USA) were isolated from the ethanol extract of the stems of *M. pachyloba*.

Pachyvone A (1)

White powder; ultraviolet (UV) (MeOH) λ_{\max} (log ϵ) 262 (4.18), 326 (2.97) nm; Infrared (IR) (KBr) ν_{\max} 3028, 2910, 1673, 1456, 834 cm⁻¹. Both ¹H nuclear magnetic resonance (NMR) and ¹³C NMR data are shown in Table 1; high-resolution electrospray ionization mass spectroscopy (HRESIMS) m/z 381.1707 [M+H]⁺ (calcd for C₂₃H₂₅O₅, 381.1702).

Pachyvone B (2)

White powder; UV (MeOH) λ_{\max} (log ϵ) 263 (3.64), 326 (3.07) nm; IR (KBr) ν_{\max} 3019, 2917, 1682, 1462, 863, 845 cm⁻¹. Both ¹H NMR and ¹³C NMR data are shown in Table 1; HRESIMS m/z 395.1506 [M+H]⁺ (calcd for C₂₃H₂₃O₆, 395.1495).

Pachyvone C (4)

White powder; UV (MeOH) λ_{\max} (log ϵ) 255 (3.38), 298 (2.87) nm; IR (KBr) ν_{\max} 3025, 2921, 1679, 1443, 865 cm⁻¹. Both ¹H NMR and ¹³C NMR data are shown in Table 1; HRESIMS m/z 441.1914 [M+H]⁺ (calcd for C₂₅H₂₉O₇, 441.1913).

Pachyvone D (5)

Yellowish powder; UV (MeOH) λ_{\max} (log ϵ) 266 (3.76) nm; IR (KBr) ν_{\max} 3593, 3016, 2934, 1688, 1459, 827 cm⁻¹. Both ¹H NMR

and ¹³C NMR data are shown in Table 1; HRESIMS m/z 443.1705 [M+H]⁺ (calcd for C₂₄H₂₇O₈, 443.1706).

Pachyvone E (6)

Yellowish powder; UV (MeOH) λ_{\max} (log ϵ) 264 (3.58), 294 (2.92) nm; IR (KBr) ν_{\max} 3598, 3023, 2928, 1663, 1466, 831 cm⁻¹. Both ¹H NMR and ¹³C NMR data are shown in Table 1; HRESIMS m/z 413.1605 [M+H]⁺ (calcd for C₂₃H₂₅O₇, 413.1600).

Pachythone A (7)

Yellow powder; UV (MeOH) λ_{\max} (log ϵ) 287 (4.18), 340 (2.17) nm; IR (KBr) ν_{\max} 3604, 2894, 1664, 1456, 848, 715 cm⁻¹. Both ¹H NMR and ¹³C NMR data are shown in Table 2; HRESIMS m/z 371.1137 [M+H]⁺ (calcd for C₂₀H₁₉O₇, 371.1131).

Cell culture and transfection

GFP-LC3-HeLa (HeLa cells stably expressing GFP-LC3) were established as previously reported [16,17]. HeLa, HepG2, MCF-7, Hct116, MDA-MB-231, and HUVECs were obtained from KeyGEN Biotech Co. (Nanjing, China) and cultured with Dulbecco's Modified Eagle Medium containing 10% fetal bovine serum and 1% penicillin/streptomycin. Cells were cultured at 37 °C in a humidified atmosphere, and the concentration of CO₂ was set at 5%.

Cytotoxicity assay

The cytotoxic effects of the isolated compounds were investigated using the 3-(4,5-dimethyl-2-thiazolyl)-2,5-diphenyl-2-H-tetrazolium bromide (MTT) assay. Briefly, cells were plated in 96-well plates with 1 × 10⁴ cells per well. Cells were cultured for 24 h before treatment with different compounds at various concentrations (0–40 μM) for 72 h. Then, 20 μL MTT solution (5 mg/mL) was added to each well and incubated for another 4 h. The supernatants were discarded, and 150 μL dimethyl sulfoxide (DMSO) was added to each well and incubated for 10 min. The absorbance

Table 1

¹H and ¹³C NMR spectroscopic data for compounds **1**, **2**, **4**–**6**^a (400 and 100 MHz for ¹H and ¹³C NMR, CDCl₃).

Position	1		2		4		5		6	
	δ_C	δ_H (J in Hz)	δ_C	δ_H (J in Hz)	δ_C	δ_H (J in Hz)	δ_C	δ_H (J in Hz)	δ_C	δ_H (J in Hz)
2	152.3	8.02, s	152.5	8.01, s	154.5	8.05, s	155.4	7.97, s	155.2	7.94, s
3	123.9		124.1		120.9		119.8		119.9	
4	176.1		175.9		176.0		181.8		181.4	
4a	120.7		120.7		120.8		108.6		105.8	
5	103.8	7.60, s	103.9	7.59, s	103.9	7.59, s	152.5		160.9	
6	151.1		151.2		151.0		136.6		95.1	6.41, s
7	151.9		151.9		151.8		157.1		162.7	
8	124.7		124.7		124.7		113.0		107.8	
8a	150.0		149.9		149.9		150.4		154.6	
1'	124.5		125.9		112.5		110.0		109.9	
2'	130.1	7.52, d (8.8)	122.3	7.00, dd (8.0, 1.6)	151.9		152.4		152.5	
3'	113.9	6.98, d (8.8)	108.4	6.87, d (8.0)	98.3	6.63, s	100.0	6.67, s	100.0	6.66, s
4'	159.5		147.6		149.8		146.9		146.8	
5'	113.9	6.98, d (8.8)	147.6		143.1		140.4		140.4	
6'	130.1	7.52, d (8.8)	109.8	7.12, d (1.6)	115.3	6.96, s	114.4	6.87, s	114.4	6.88, s
7'			101.1	5.99, s						
1''	22.9	3.59, d (7.2)	22.9	3.59, d (7.2)	23.0	3.60, d (7.2)	22.2	3.46, d (7.2)	21.5	3.42, d (7.2)
2''	121.5	5.21, t (7.2)	121.5	5.21, t (7.2)	121.6	5.23, t (7.2)	122.2	5.18, t (7.2)	122.1	5.17, t (7.2)
3''	132.7		132.7		132.6		132.1		131.9	
4''	17.9	1.84, s	17.9	1.84, s	17.9	1.84, s	17.8	1.81, s	17.8	1.79, s
5''	25.8	1.69, s	25.8	1.69, s	25.8	1.70, s	25.8	1.70, s	25.8	1.68, s
6-OCH ₃	56.0	3.96, s	56.1	3.96, s	56.0	3.96, s	60.7	3.93, s		
7-OCH ₃	61.1	3.93, s	61.1	3.93, s	61.1	3.93, s	61.4	4.01, s	56.1	3.90, s
2'-OCH ₃					56.9	3.79, s	56.5	3.74, s	56.5	3.75, s
4'-OCH ₃	55.3	3.84, s			56.2	3.94, s				
5'-OCH ₃					56.6	3.86, s	56.7	3.86, s	56.7	3.86, s

^a Chemical shifts are given in ppm. J values (Hz) are given in parentheses. Assignments were made based on the analysis of ¹H–¹H COSY, HSQC, and HMBC data.

Table 2
¹H and ¹³C NMR spectroscopic data for compound **7**^a (400 and 100 MHz for ¹H and ¹³C NMR, CDCl₃).

position	7	
	δ_C	δ_H
1	156.9	
2	95.1	6.40, s
3	160.5	
4	104.7	
4a	157.5	
5	139.8	
6	145.6	
7	145.5	
8	103.6	7.47, s
8a	116.5	
9	180.1	
9a	103.3	
10a	145.1	
4'	115.5	6.73, d (10.0)
5'	127.5	5.60, d (10.0)
6'	78.2	
7'	28.4	1.48, s
8'	28.4	1.48, s
5-OCH ₃	61.9	4.05, s
6-OCH ₃	61.5	4.16, s

^a Chemical shifts are given in ppm. *J* values (Hz) are given in parentheses. Assignments were made based on the analysis of ¹H-¹H COSY, HSQC, and HMBC data.

at 570 nm was detected using a microplate reader (BioTek, Winooski, USA). The cytotoxicity (IC₅₀, half maximal inhibitory concentration) of each compound was calculated using GraphPad Prism 5.

Autophagy detection using GFP-LC3 expression in HeLa cells

The effects of compound-induced autophagy were determined in GFP-LC3-HeLa cells [16,17]. The GFP-LC3-HeLa cells were plated in 24-well plates and incubated with the tested compounds at various concentrations. Chloroquine phosphate treatment-induced LC3 dots were used as an observation control. Plates were incubated for 24 h, and the GFP-LC3 puncta were detected and imaged under a fluorescence microscope (Olympus, Tokyo, Japan) with Olympus Stream software.

Detection of apoptotic cells using flow cytometry

HeLa and MCF-7 cells seeded on six-well plates for 24 h were incubated with 0, 2.5, 5, 10, and 20 μ M compound **9** or colchicine (positive control) for 48 h. Cells were collected, digested with ethylenediaminetetraacetic acid-free trypsin for 3 min and centrifuged (170 \times g, 3 min) before being washed with phosphate buffered saline (PBS) buffer twice and centrifuged (170 \times g, 3 min). Then, the cells were resuspended and stained with reagents from the Annexin V/propidium iodide (PI) Apoptosis Detection Kit (Invitrogen) for approximately 30 min according to the manufacturer's instructions. The stained cells were subjected to flow cytometry (Attune NxT, Life Technology, Waltham, USA) for analysis. Data and image analyses were conducted using FlowJo 7.6 software. The PI- / Annexin V-, PI+ / Annexin V-, PI- / Annexin V+, and PI+ / Annexin V+ cells were considered viable cells, necrotic cells, early apoptotic cells, and late apoptotic cells, respectively. In this study, the early apoptotic cells and late apoptotic cells were combined and counted as the total number of apoptotic cells.

Western blotting analysis

HeLa cells were collected and washed twice with PBS before being lysed with protein lysis radioimmunoprecipitation assay

buffer for 30 min at 4 °C. Samples were subjected to centrifugation at 18894g for 30 min at 4 °C. The supernatants were collected, and the protein concentration was determined using a bicinchoninic acid assay (Thermo Scientific, Waltham, USA). Proteins were denatured in 1 \times loading buffer in boiling water for 10 min. Equal amounts (20 μ g) of samples were loaded onto sodium dodecyl sulfate polyacrylamide gel electrophoresis for the ionophoretic separation of proteins for 1 h using a constant voltage of 120 V. Proteins in the gel were transferred to polyvinylidene difluoride (PVDF) membranes using 260 mA constant current for 2 h. Transferred PVDF membranes were blocked with a 5% milk solution (in 1 \times PBST buffer (0.1% Tween[®] 20 in PBS buffer)) for 1 h at room temperature before incubation with primary antibodies at 4 °C overnight. PVDF membranes were washed three times (10 min each) with 1 \times PBST buffer. Secondary antibodies were incubated with PVDF membranes for 45 min at room temperature, and the membranes were washed three times (10 min each) with 1 \times PBST. The membranes were stained with enhanced chemiluminescence reagents (Millipore, Burlington, USA) and imaged using a chemiluminescence image analysis system (Tianneng, Shanghai, China) with Tanon-5200 Multi software (Tianneng, Shanghai, China).

Results and discussion

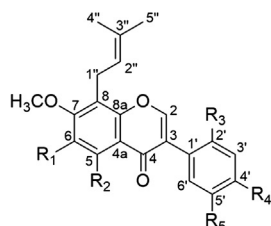
Isolation of compounds 1–28.

Approximately 10 kg dry stems of *M. pachyloba* were shattered into powder (approximately 20-mesh) and extracted with 95% aqueous EtOH three times. The EtOH extracts were combined, evaporated to dryness, suspended in H₂O and successively extracted with petroleum ether and CH₂Cl₂. The petroleum ether and CH₂Cl₂ extracts were further separated using column chromatography (silica gel and Sephadex LH-20) as well as reverse-phase SP-HPLC to obtain compounds **1–28** (see Fig. 1).

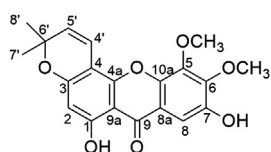
Chemical structure identification of the isolated compounds.

Compound **1** was obtained as a white powder and assigned a molecular formula of C₂₃H₂₄O₅ by HRESIMS at *m/z* 381.1707 ([M+H]⁺, calcd for 381.1702), indicating twelve double bond equivalents. The UV spectrum absorption at 256 and 326.4 nm, ¹H (δ_H 8.02 for H-2) and ¹³C (δ_C 152.3 for C-2) NMR spectra and ¹H detected heteronuclear multiple bond correlation (HMBC) correlations (Fig. 2) of H-2 (δ_H 8.02) to C-3 (δ_C 123.9), C-8a (δ_C 150.0) and C-4 (δ_C 176.1) showed this compound to be an isoflavone-type skeleton [18,19]. Analysis of the ¹H NMR (Table 1) and homonuclear chemical shift correlation spectroscopy (COSY) correlations revealed a γ , γ -dimethylallyl unit [δ_H 3.59 (2H, d, *J* = 7.2 Hz), 5.21 (1H, t, *J* = 7.2 Hz), 1.84 (3H, s), 1.69 (3H, s)], a 1,4-disubstituted benzene ring [δ_H 7.52 (2H, d, *J* = 8.8 Hz), 6.98 (2H, d, *J* = 8.8 Hz)], three methoxy groups [δ_H 3.96 (3H, s), 3.93 (3H, s), 3.84 (3H, s)], an aromatic proton [δ_H 7.60 (1H, s)] and a vinyl proton [δ_H 8.02 (1H, s)]. The ¹³C NMR spectra of **1** indicated 23 signals, including three methoxy groups [δ_C 55.3, 56.0 and 61.1] and one γ , γ -dimethylallyl unit [δ_C 17.9, 22.9, 25.8, 121.5 and 132.7]. Comparison of the NMR data of **1** and millesianin H [2] revealed similar carbon and proton resonances, except that **1** contained one more methoxy group. A further HMBC correlation study (Fig. 2) showed that this methoxy group (δ_H 3.93) was attached to C-7 (δ_C 151.9). Therefore, the chemical structure of compound **1** was identified as 8-(γ , γ -dimethylallyl)-6,7,4'-trimethoxyisoflavone, and it was named pachyvone A.

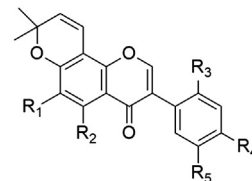
Compound **2** was isolated as a white powder. Its formula of C₂₃H₂₂O₆ was deduced by HRESIMS at *m/z* 395.1506 ([M+H]⁺, calcd for 395.1495). In the ¹H and ¹³C NMR spectra of **2**, an olefinic



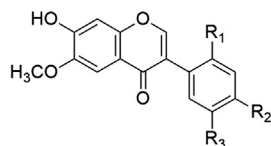
- 1 $R_1 = \text{OCH}_3, R_2 = \text{H}, R_3 = \text{H}, R_4 = \text{OCH}_3, R_5 = \text{H}$
 2 $R_1 = \text{OCH}_3, R_2 = \text{H}, R_3 = \text{H}, R_4, R_5 = -\text{OCH}_2\text{O}-$
 3 $R_1 = \text{OCH}_3, R_2 = \text{H}, R_3 = \text{OCH}_3, R_4, R_5 = -\text{OCH}_2\text{O}-$
 4 $R_1 = \text{OCH}_3, R_2 = \text{H}, R_3 = R_4 = R_5 = \text{OCH}_3$
 5 $R_1 = \text{OCH}_3, R_2 = \text{OH}, R_3 = \text{OCH}_3, R_4 = \text{OH}, R_5 = \text{OCH}_3$
 6 $R_1 = \text{H}, R_2 = \text{OH}, R_3 = \text{OCH}_3, R_4 = \text{OH}, R_5 = \text{OCH}_3$



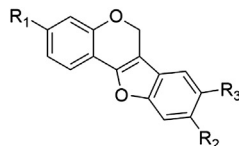
7



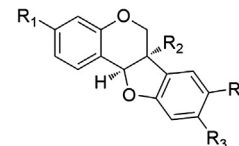
- 8 $R_1 = \text{OCH}_3, R_2 = \text{H}, R_3 = \text{H}, R_4 = \text{OCH}_3, R_5 = \text{H}$
 9 $R_1 = \text{OCH}_3, R_2 = \text{H}, R_3 = \text{H}, R_4, R_5 = -\text{OCH}_2\text{O}-$
 10 $R_1 = \text{OCH}_3, R_2 = \text{H}, R_3 = \text{H}, R_4 = R_5 = \text{OCH}_3$
 11 $R_1 = \text{OCH}_3, R_2 = \text{H}, R_3 = \text{OCH}_3, R_4, R_5 = -\text{OCH}_2\text{O}-$
 12 $R_1 = \text{OCH}_3, R_2 = \text{H}, R_3 = R_4 = R_5 = \text{OCH}_3$
 13 $R_1 = \text{H}, R_2 = \text{OH}, R_3 = R_4 = R_5 = \text{OCH}_3$



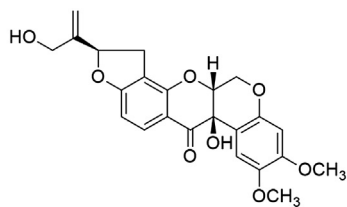
- 14 $R_1 = \text{H}, R_2 = R_3 = \text{OCH}_3$
 15 $R_1 = \text{OCH}_3, R_2, R_3 = -\text{OCH}_2\text{O}-$
 16 $R_1 = R_2 = R_3 = \text{OCH}_3$



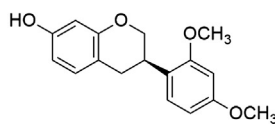
- 17 $R_1 = \text{OH}, R_2 = \text{OH}, R_3 = \text{H}$
 18 $R_1 = \text{OH}, R_2, R_3 = -\text{OCH}_2\text{O}-$
 19 $R_1 = \text{OCH}_3, R_2, R_3 = -\text{OCH}_2\text{O}-$



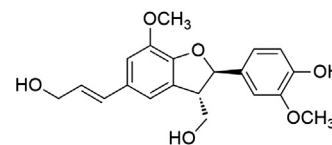
- 20 $R_1 = \text{OH}, R_2 = \text{H}, R_3 = \text{OCH}_3, R_4 = \text{H}$
 21 $R_1 = \text{OH}, R_2 = \text{H}, R_3, R_4 = -\text{OCH}_2\text{O}-$
 22 $R_1 = \text{OCH}_3, R_2 = \text{OH}, R_3 = \text{OCH}_3, R_4 = \text{H}$
 23 $R_1 = \text{OCH}_3, R_2 = \text{OH}, R_3, R_4 = -\text{OCH}_2\text{O}-$



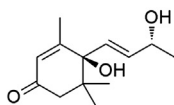
24



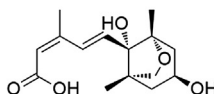
25



26

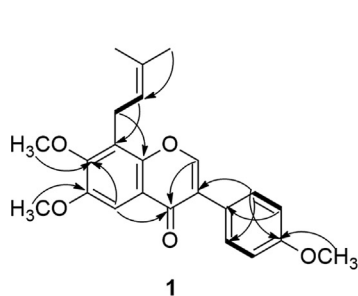


27

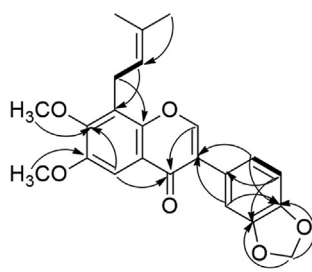


28

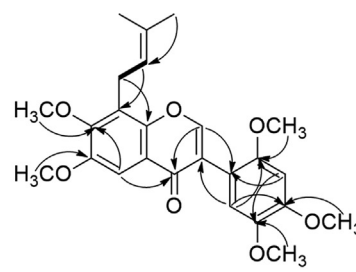
Fig. 1. Structures of compounds 1–28.



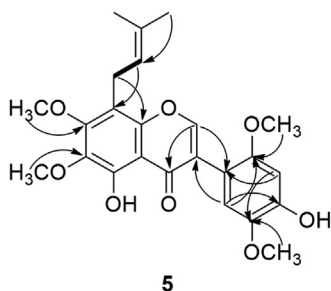
1



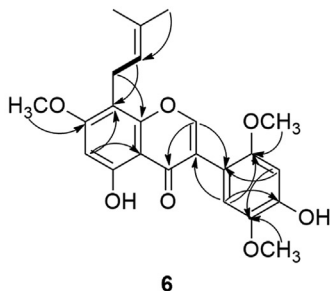
2



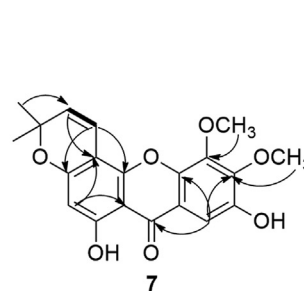
4



5



6



7

— COSY
 ↷ HMBC

Fig. 2. Key COSY and HMBC correlations of compounds 1, 2, and 4–7.

proton at δ_H 8.01 (s, H-2), an oxygenated carbon resonance at δ_C 152.5 (C-2) and a carbonyl carbon resonance at δ_C 175.9 (C-4) suggested an isoflavone skeleton [18,19]. The 1H NMR spectrum showed (Table 1) the presence of a γ , γ -dimethylallyl unit [δ_H 3.59 (2H, d, $J = 7.2$ Hz), 5.21 (1H, t, $J = 7.2$ Hz), 1.84 (3H, s), 1.69 (3H, s)], an ABX-type benzene ring [δ_H 6.87 (1H, d, $J = 8.0$ Hz), 7.00 (1H, dd, $J = 8.0$ Hz, $J = 1.6$ Hz), 7.12 (1H, d, $J = 1.6$ Hz)], two methoxy groups [δ_H 3.96 (3H, s), 3.93 (3H, s)], a methylenedioxy group [δ_H 5.99 (2H, s)], an aromatic proton [δ_H 7.59 (1H, s)] and a vinyl proton [δ_H 8.01 (1H, s)]. The ^{13}C NMR spectra of **2** indicated 23 signals, including two methoxy groups [δ_C 56.1 and 61.1], one γ , γ -dimethylallyl unit [δ_C 17.9, 22.9, 25.8, 121.5, and 132.7] and a methylenedioxy functionality [δ_C 101.1]. These signals were similar to the resonances of predurmillone [20], except that the hydroxyl group in predurmillone was replaced by a methoxyl group (δ_H 3.93) in **2**. These results were further directly supported by the HMBC correlation (Fig. 2) from the proton signal at δ_H 3.93 to C-7 (δ_C 151.96) and indirectly demonstrated by the HMBC correlations (Fig. 2) from the proton signals at δ_H 7.59 (s) to C-7 (δ_C 151.96) and C-4 (δ_C 175.9) because this proton was not substituted and the methoxyl group (δ_H 3.93) should be attached to C-7. Therefore, the structure of compound **2** was identified as 8-(γ , γ -dimethylallyl)-6,7-dimethoxy-4',5'-methylenedioxyisoflavone, and it was named pachyvone B.

Compound **4** was isolated as a white powder and assigned the molecular formula $C_{25}H_{28}O_7$, as indicated by the HRESIMS at m/z 441.1914 ($[M+H]^+$, calcd for 441.1913), which suggested twelve

double bond equivalents. A singlet at δ_H 8.05 (H-2) in the 1H NMR spectrum and the ^{13}C NMR signals at δ_C 154.5 (C-2), 120.9 (C-3), and 176.0 (C-4) were consistent with an isoflavone core structure that was further corroborated by its UV spectrum (λ_{max} at 255.4 and 297.9 nm) [18,19]. Compound **4** and millesianin I [2] had similar 1H and ^{13}C NMR data (Table 1) because both compounds contained a γ , γ -dimethylallyl unit, a 1,2,4,5-tetrasubstituted benzene ring, four methoxy groups, an aromatic proton and a vinyl proton, except that compound **4** contained one additional methoxy group signal at δ_C 61.11 and δ_H 3.93. HMBC correlation (Fig. 2) of the proton resonance at δ_H 3.93 with C-7 (δ_C 151.81) demonstrated that the additional methoxy group was attached to C-7. Accordingly, the structure of compound **4** was established as 8-(γ , γ -dimethylallyl)-6,7,2',4',5'-pentamethoxyisoflavone, and it was named pachyvone C.

Compound **5** was isolated as a yellowish powder. Its molecular formula was determined to be $C_{24}H_{26}O_8$ by HRESIMS at m/z 443.1705 ($[M+H]^+$, calcd for 443.1706), suggesting twelve double bond equivalents. The UV maxima at λ_{max} 266.0 and 300.0 nm as well as the specific proton signal at δ_H 7.97 (1H, s, H-2) that was correlated with δ_C 155.4 (C-2), as shown by the heteronuclear single quantum coherence spectrum, suggested that compound **5** possessed an isoflavone-type skeleton [18,19]. The 1H NMR (Table 1) and COSY correlations of compound **5** revealed signals for a γ , γ -dimethylallyl unit [δ_H 3.46 (2H, d, $J = 7.2$ Hz), 5.18 (1H, t, $J = 7.2$ Hz), 1.81 (3H, s), 1.70 (3H, s)], a 1,2,4,5-tetrasubstituted benzene ring [δ_H 6.67 (1H, s), 6.87 (1H, s)], four methoxy groups [δ_H 4.01 (3H, s), 3.93 (3H, s), 3.86 (3H, s), 3.74 (3H, s)] and a hydroxyl group [δ_H 12.88 (1H, s)]. The ^{13}C NMR spectrum of **5** indicated 23 signals, including four methoxy groups [δ_C 56.5, 56.7, 60.7 and 61.4] and one γ , γ -dimethylallyl unit [δ_C 17.8, 22.2, 25.8, 122.2 and 132.1]. Compound **5** exhibited NMR data very similar to those of compound **4**. However, **5** had a chelated hydroxyl group at δ_H 12.88 (1H, s, OH-5), which is absent in **4**. Moreover, there is one more methoxyl group in **5** compared to **4**. The HMBC correlations of the hydroxyl group (δ_H 12.88) with C-4a (δ_C 108.60), C-5 (δ_C 152.47) and C-6 (δ_C 136.64) suggested a hydroxy group at the C-5 position. HMBC correlations from the proton signals of four methoxy groups [δ_H 4.01 (3H, s), 3.93 (3H, s), 3.86 (3H, s), 3.74 (3H, s)] demonstrated that these four methoxy groups were attached to C-7, C-6, C-5', and C-2', respectively. The chemical shift of C-4' (δ_C 146.89) combined with the molecular formula $C_{24}H_{26}O_8$ showed that compound **5** had a hydroxy group at the C-4' position. The key HMBC correlations are shown in Fig. 2. On the basis of the evidence obtained, the structure of compound **5** was determined to be 8-(γ , γ -dimethylallyl)-5,4'-dihydroxy-6,7,2',5'-tetramethoxyisoflavone, and it was named pachyvone D.

Compound **6** was obtained as a yellowish powder with the molecular formula $C_{23}H_{24}O_7$ deduced by HRESIMS at m/z

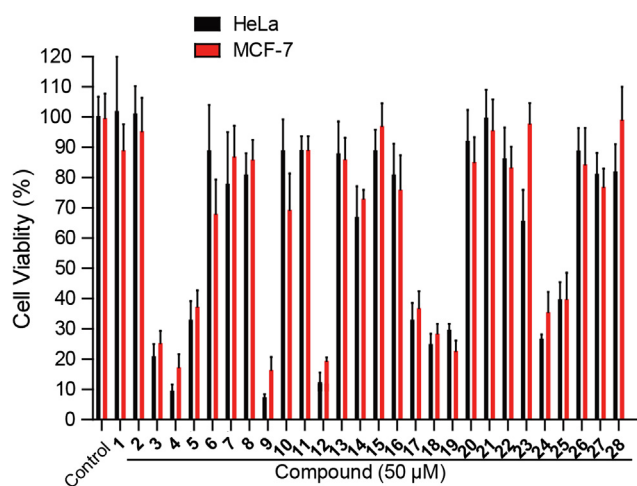


Fig. 3. Preliminary screening of active compounds on HeLa and MCF-7 cells. HeLa and MCF-7 cells were treated with 50 μ M for 72 h, and then cell viability was tested by MTT assay.

Table 3

Cytotoxicity of selected compounds against five cancer cell lines and a normal cell lines (HUVEC).^a

Compound	IC ₅₀ (μ M)					
	HeLa	HepG2	MCF-7	HCT-116	MDA-MB-231	HUVEC
3	14.56 \pm 0.54	15.97 \pm 0.67	19.61 \pm 0.66	23.21 \pm 1.22	20.78 \pm 2.35	>50
4	7.86 \pm 1.21	8.74 \pm 0.83	18.46 \pm 0.51	8.61 \pm 0.72	15.85 \pm 2.15	>50
5	35.67 \pm 3.91	31.61 \pm 2.06	35.05 \pm 1.44	25.91 \pm 0.85	27.64 \pm 4.54	>50
9	6.09 \pm 1.09	17.85 \pm 1.60	11.08 \pm 0.68	15.14 \pm 0.61	12.89 \pm 3.10	>50
12	14.82 \pm 2.12	8.05 \pm 0.90	14.37 \pm 1.84	19.78 \pm 1.29	11.09 \pm 0.91	>50
17	36.15 \pm 7.34	34.25 \pm 1.87	30.34 \pm 1.32	39.66 \pm 2.06	36.78 \pm 5.61	>50
18	22.50 \pm 1.09	13.39 \pm 1.41	21.21 \pm 0.93	21.90 \pm 1.73	25.45 \pm 2.09	>50
19	30.19 \pm 0.54	25.38 \pm 1.92	21.10 \pm 1.65	27.03 \pm 1.64	22.76 \pm 3.54	>50
24	19.89 \pm 2.09	32.61 \pm 1.84	33.12 \pm 1.93	16.65 \pm 0.82	27.16 \pm 3.25	>50
25	40.12 \pm 4.32	28.61 \pm 2.90	36.42 \pm 2.08	31.90 \pm 1.52	33.45 \pm 2.33	>50
Doxorubicin	0.03 \pm 0.001	0.02 \pm 0.002	0.02 \pm 0.003	0.03 \pm 0.003	0.03 \pm 0.002	0.04 \pm 0.005

^a Results are presented as means \pm SEM (n = 3).

413.1605 ($[(M+H)^+]$, calcd for 413.1600). The UV maxima at λ_{max} 263.7 and 294.4 nm along with the IR absorptions (ν_{max}) at 1663 and 1466 cm^{-1} showed this compound to be an isoflavonoid, as supported by the characteristic ^1H and ^{13}C NMR resonances at $\delta_{\text{H}-2}$ 7.94 and $\delta_{\text{C}-2}$ 155.2 for this type of natural product [18,19]. The NMR data (Table 1) were very similar to those of compound 5, except for the loss of one methoxy group signal and the appearance of one additional aromatic proton signal at δ_{C} 95.12 and δ_{H} 6.41, which indicates that one methoxy group of compound 5 may be replaced by an aromatic proton to obtain compound 6. The HMBC correlations (Fig. 2) from the aromatic proton signal at δ_{H} 6.41 to C-4a (δ_{C} 105.83), C-5 (δ_{C} 160.93), C-7 (δ_{C} 162.72) and C-8 (δ_{C} 107.82) suggested that the aromatic proton was attached to C-6. Therefore, compound 6 was determined to be 8-(γ , γ -dimethylallyl)-5,4'-dihydroxy-7,2',5'-trimethoxyisoflavone, and it was named pachyvone E.

The physical nature of isoflavones has a close relationship with their structure. In these newly isolated isoflavones, compounds 1, 2, and 4 were reported as white powders, while compounds 5 and 6 were reported as yellow powders. Careful investigation of the differences in structures revealed that the presence of a 4-OH

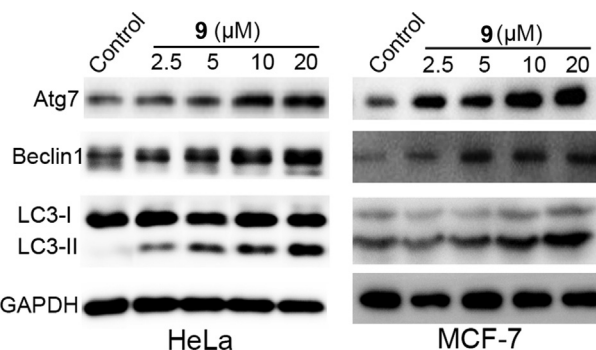


Fig. 5. Compound 9 induced autophagy in HeLa and MCF-7 cells. HeLa and MCF-7 cells were treated with the indicated concentrations of compound 9 for 24 h. Western blottings were used to measure the protein levels of LC3, Beclin1, and Atg7. GAPDH was used as a loading control.

group in the yellow-colored compounds (5 and 6) could verify the extended conjugation system, while this 4-OH moiety is absent or replaced in the white-colored compounds.

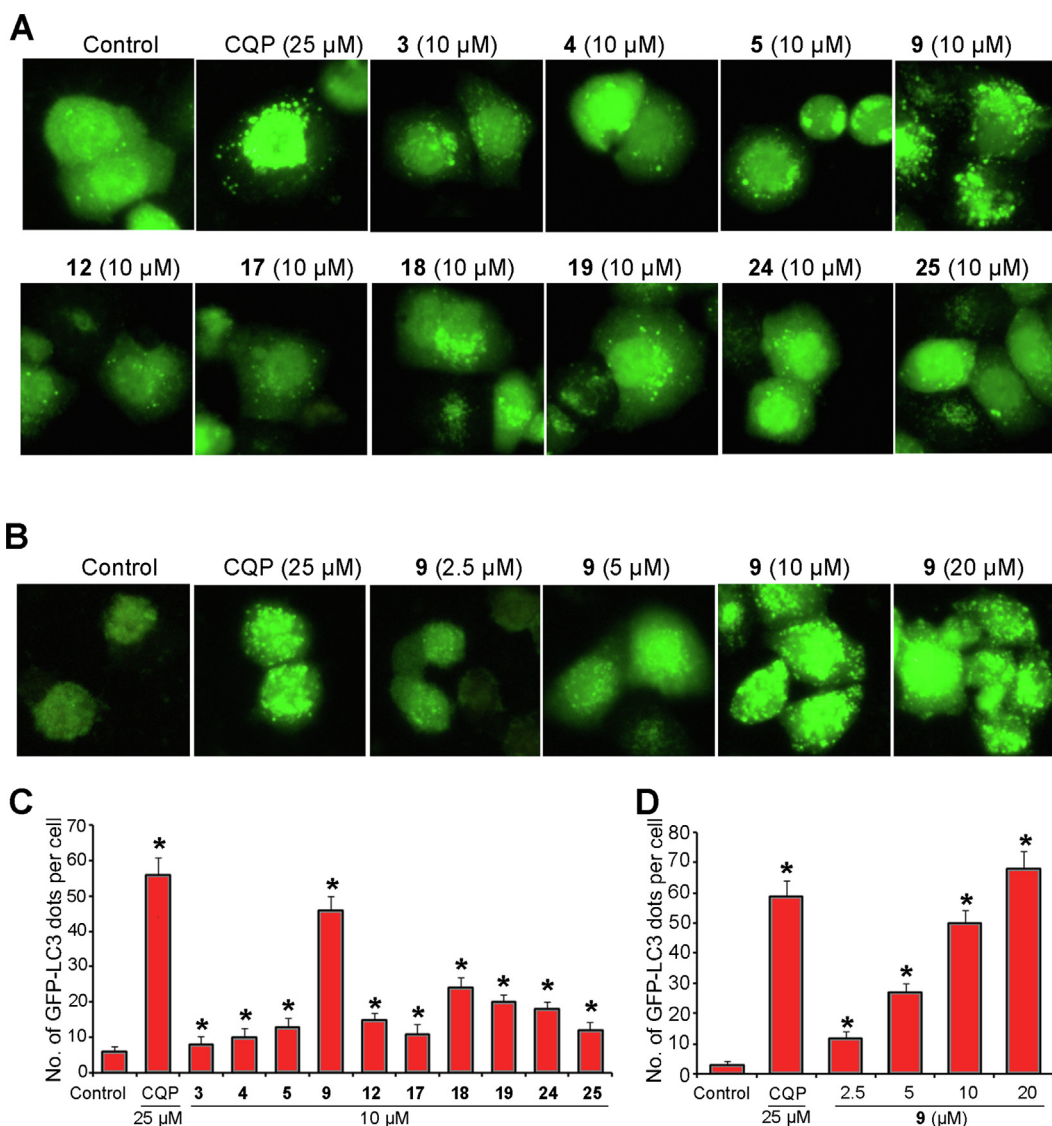


Fig. 4. Selected compounds isolated from *M. pachyloba* induced autophagy. A. HeLa cells stably expressing GFP-LC3 (GFP-LC3-HeLa) were treated with ten compounds (3–5, 9, 12, 17–19, 24, and 25) at 10 μM or with chloroquine phosphate (CQP) at 25 μM for 24 h. B. GFP-LC3-HeLa cells were treated with compound 9 at 2.5, 5, 10, and 20 μM or chloroquine phosphate at 25 μM for 24 h. C and D. The number of GFP-LC3 dots/cell was quantified.

Compound **7** was obtained as a yellow powder, and its molecular formula was assigned as $C_{20}H_{18}O_7$ from the positive ion peak at m/z 371.1137 ($[M+H]^+$, calcd for 371.1131) in the HRESIMS, which corresponded to twelve double bond equivalents. The 1H NMR spectrum (Table 2) showed similar signals to nigrolineaxanthone F [21]: two aromatic protons [δ_H 6.40 (1H, s) and 7.47 (1H, s)]

and dimethylchromene protons [δ_H 5.60 (1H, d, $J = 10.0$ Hz), 6.73 (1H, d, $J = 10.0$ Hz) and 1.48 (6H, s)]. These protons were located at the same positions as nigrolineaxanthone F according to their HMBC correlations. The major difference between compound **7** and nigrolineaxanthone F was that compound **7** exhibited two more methoxy group signals at δ_H 4.05 and 4.16 and nigrolineax-

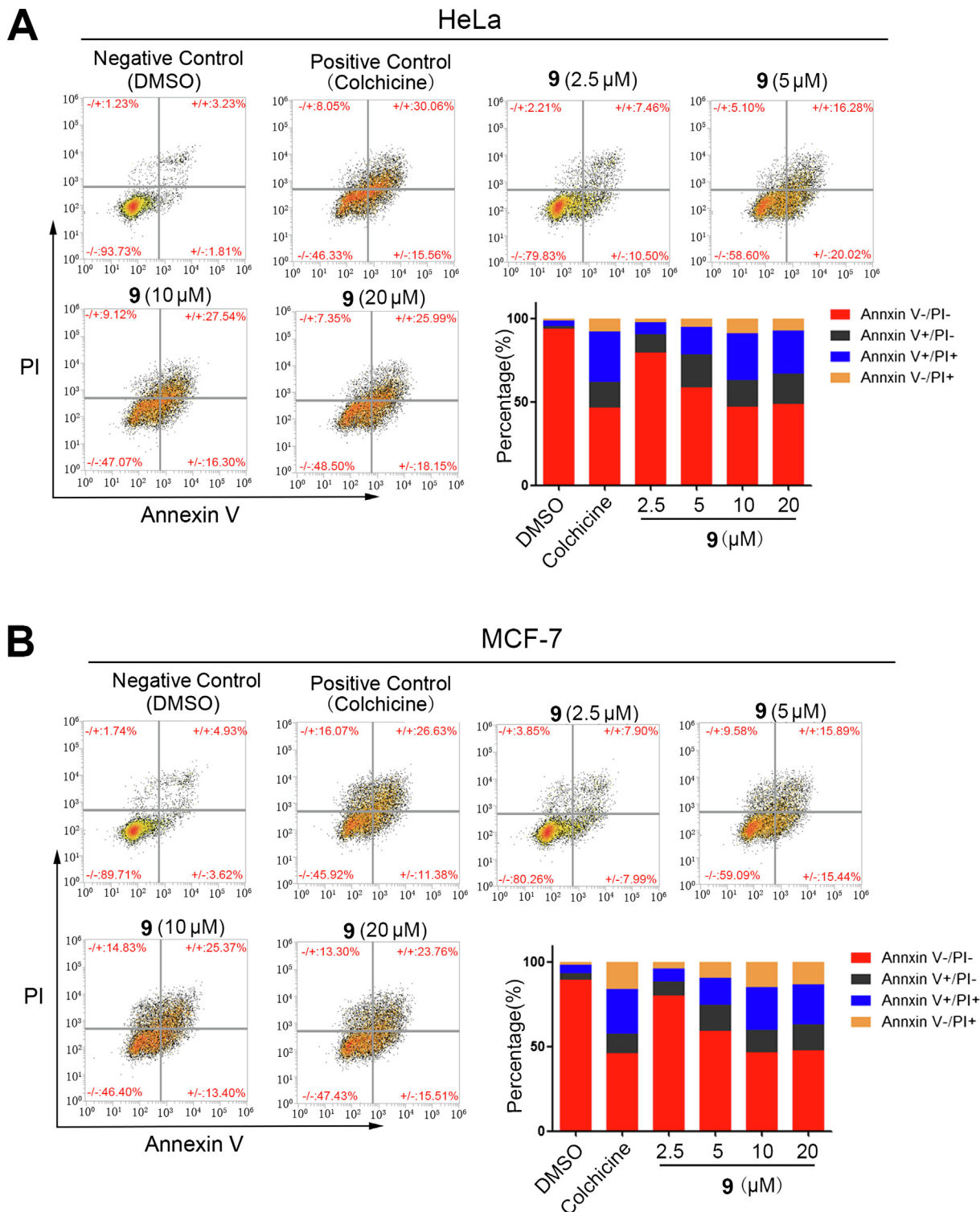


Fig. 6. Quantitative analysis of apoptosis using the Annexin V/PI double-staining assay and flow cytometry calculations. (A) HeLa cells were treated with compound **9** at different concentrations (0, 2.5, 5.0, 10.0, and 20.0 μ M) or 1 μ M colchicine for 48 h; the histogram shows the percentages of viable cells (PI-/Annexin V-), necrotic cells (PI+/Annexin V-), early apoptotic cells (PI-/Annexin V+), and late apoptotic cells (PI+/Annexin V+). (B) MCF-7 cells were treated with compound **9** at different concentrations (0, 2.5, 5.0, 10.0, and 20.0 μ M) or 1 μ M colchicine for 48 h; the histogram shows the percentages of viable cells (PI-/Annexin V-), necrotic cells (PI+/Annexin V-), early apoptotic cells (PI-/Annexin V+), and late apoptotic cells (PI+/Annexin V+).

anthon F had two more vinyl signals at δ_H 7.39 (1H, d, $J = 8.5$ Hz) and 7.28 (1H, dd, $J = 8.5$ Hz, $J = 3.0$ Hz), which suggests that the vinyl protons were substituted by these two methoxy groups. This result was corroborated by the HMBC correlations (Fig. 2) from the proton resonance at δ_H 7.47 (H-8) to C-6 (δ_C 145.6). Therefore, the structure of compound **7** was determined to be 1,7-dihydroxy-5,6-dimethoxy-6',6'-dimethylpyrano (2',3':3,4) xanthone, and it was named pachythone A.

Based on the spectroscopic data and comparisons with the data found in the literature, the known compounds were identified as 8-prenylmilturone (**3**) [22], 6-methoxycalopogonium isoflavone A (**8**) [23], durmillone (**9**) [24], durallone (**10**) [25], ichthyone (**11**) [8], millesianin C (**12**) [26], toxicarol isoflavone (**13**) [27], cladrastin (**14**) [28], dalpatein (**15**) [29], 7-hydroxy-2',4',5',6-tetramethoxyisoflavone (**16**) [30], 3,9-dihydroxypterocarp-6a-en (**17**) [31], dehydromaackiain (**18**) [32], flemichapparin B (**19**) [33], (-)-medicarpin (**20**) [34], (-)-maackiain (**21**) [35], (-)-variabilin (**22**) [36], (-)-pisatin (**23**) [37], dalbinol (**32**) [38], (-)-sativin (**25**) [39], (-)-dehydrodiconiferyl alcohol (**26**) [40], (+)-vomifoliol (**27**) [41], and dihydrophaseic acid (**28**) [42].

Primary screening for cytotoxic compounds

Flavones have shown cytotoxic activity toward cancer cells such as HeLa and MCF-7 cell lines [43,44]. Therefore, the primary cytotoxic activities of 28 compounds were tested on HeLa and MCF-7 cells by MTT assay. As shown in Fig. 3, ten compounds (**3–5**, **9**, **12**, **17–19**, **24**, and **25**) showed growth inhibition of HeLa and MCF-7 cells at a 50 μ M concentration, while the other compounds possessed no activity. Notably, compounds **4**, **9**, and **12** are the most active compounds.

Cytotoxic activities of selected compounds on cancer cells and normal cells

Isoflavones are known to be phytoestrogens, and thus, an estrogen receptor-positive cell line (MCF-7) and estrogen receptor-negative cell line (MDA-MB-231) together with other cancer cell lines were used in this study. The cytotoxic activities of the ten active compounds were evaluated in five cancer cell lines (HeLa, HepG2, MCF-7, Hct116, and MDA-MB-231) and one normal cell line (HUVEC) using doxorubicin as a positive control. Cancer cells were treated with increasing concentrations of the compounds (0, 2.5, 5, 10, 20, and 40 μ M), and normal cells were treated with the compounds at 50 μ M for 72 h. Cell viability was examined by the MTT assay. The IC_{50} values of the ten compounds were calculated and are presented in Table 3. Compounds **4**, **9**, and **12** showed better anticancer activities than the other compounds. These compounds showed no selectivity on estrogen receptor-negative and estrogen receptor-positive cells, implying that these compounds exhibit no activity on estrogen receptors. Notably, all of these

compounds had no activity against normal cells, suggesting that these compounds are safe anticancer candidate compounds.

Compound 9 induced autophagy in HeLa and MCF-7 cells

Numerous flavonoids mediate cell death using an autophagy-dependent pathway [45–47]. Here, a GFP-LC3-HeLa cell line was used to investigate whether the cytotoxicity of the ten compounds was associated with autophagy. LC3 is an autophagy marker protein that forms autophagosomes during autophagy induction [48]. Autophagosome dots, indicating aggregated LC3 protein, were directly observed in GFP-LC3-HeLa cells stably expressing GFP-labeled LC3 proteins using a fluorescence microscope. GFP-LC3-HeLa cells were treated with the ten compounds for 24 h at 10 μ M. Chloroquine phosphate treatment-induced LC3 dots were used as the observation control. Fig. 4 shows that chloroquine phosphate induced an obvious increase in the GFP-LC3 dots, which indicates the appearance of autophagosomes. All the tested compounds produced an increase in GFP-LC3 dots, and compound **9** (durmillone) showed the best activity. Durmillone (**9**) induced GFP-LC3 punctation in a dose-dependent manner. These results suggest that the ten compounds induce autophagy and that compound **9** exhibits the best activity.

The expression of autophagy-associated proteins, such as LC3-II, Beclin1, and Atg7 [48], was detected in HeLa and MCF-7 cells treated with compound **9** using Western blotting analysis, further verifying this result. The results indicated that compound **9** remarkably and dose-dependently upregulated the expression levels of LC3-II, Beclin1, and Atg7 in HeLa and MCF-7 cells (Fig. 5). Taken together, these results demonstrate that compound **9** induced obvious autophagy in HeLa cells. As compound **9** exhibited the best activity in inducing autophagy, it was chosen for further study.

Compound 9 induced apoptosis in HeLa and MCF-7 cells.

Plasma membrane surface Annexin V is a marker of apoptosis, and propidium iodide (PI) is used to detect late apoptotic cells, so the combined PI/Annexin V double staining method is a classic method of apoptosis detection. In the present study, the PI/Annexin V double staining flow cytometric assay was used to further investigate compound **9** induction of apoptosis in cancer cells. Colchicine, a tubulin inhibitor, was employed as a positive control. The results revealed that compound **9** induced apoptosis in HeLa and MCF-7 cells in a concentration-dependent manner. The apoptosis rates were 5.04%, 45.62%, 17.96%, 36.30%, 43.84%, and 44.14% for HeLa cells treated with the negative control (DMSO), positive control (colchicine), and 2.5, 5, 10 and 20 μ M compound **9**, respectively. Additionally, the apoptosis rates in MCF-7 cells were 8.55%, 38.01%, 15.89%, 31.33%, 38.77%, and 39.27% for the negative control (DMSO), positive control (colchicine), and 2.5, 5, 10 and 20 μ M compound **9**, respectively (Fig. 6).

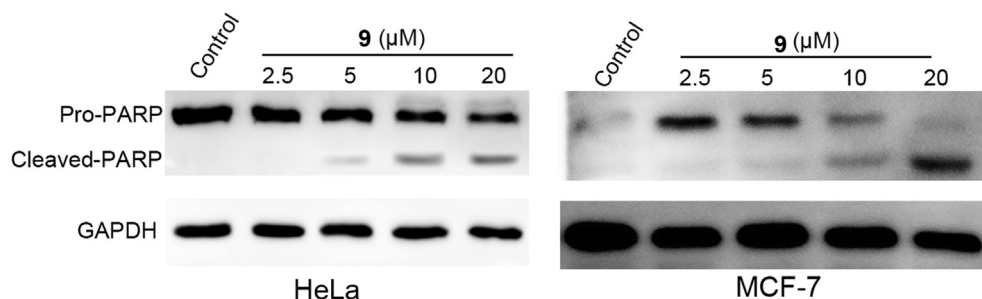


Fig. 7. Compound **9** induced apoptosis in HeLa and MCF-7 cells. HeLa and MCF-7 cells were treated with the indicated concentrations of compound **9** for 48 h. Western blotting was used to measure protein levels of PARP. GAPDH was used as a loading control.

To further verify the induction of apoptotic events by compound **9** in cancer cells, the level of poly ADP-ribose polymerase (PARP) cleavage, which is a marker of late apoptotic events, was determined using Western blotting in HeLa and MCF-7 cells. Cells treated with 2.5, 5, 10 and 20 μM compound **9** for 48 h induced obvious PARP cleavage in a concentration-dependent manner (Fig. 7), which further demonstrates that compound **9** also induces apoptosis in cancer cells.

In summary, the results of the present study suggest that compound **9** mediates cytotoxic activity through the combined action of apoptosis and autophagy.

Conclusions

In this study, systematic separation and subsequent pharmacological activity studies were carried out to obtain cytotoxic natural products from the dried stems of *M. pachyloba*. Ten cytotoxic natural products (**3–5**, **9**, **12**, **17–19**, **24**, and **25**) from the dried stems of *Millettia pachyloba* Drake were obtained, and compound **9** exhibited the highest cytotoxic activity through the combined action of apoptosis and autophagy.

Phytochemical investigation of the stems of *Millettia pachyloba* led to the isolation of five previously undescribed isoflavones (**1**, **2**, and **4–6**), one previously undescribed xanthone (**7**), and twenty-two known compounds. These findings enrich the diversity of chemical components of the genus *Millettia*. Biological assays to examine the cytotoxic effects of ten compounds (**3–5**, **9**, **12**, **17–19**, **24**, and **25**) showed that these compounds produced cytotoxic effects in HepG2, MCF-7, and HeLa cell, with IC_{50} values ranging from 5 to 40 μM . Notably, durmillone (**9**) induced cytotoxicity through the combined action of apoptosis and autophagy in HeLa cells, which suggests that flavonoids are responsible for the cytotoxicity of *M. pachyloba*.

Conflict of interest

The authors have declared no conflict of interest.

Compliance with Ethics Requirements

This article does not contain any studies with human or animal subjects.

Acknowledgments

This study acknowledges grant support from the National Natural Science Foundation of China (81874297, 81803021 and 81527806), the 1.3.5 Project for Disciplines of Excellence, West China Hospital, Sichuan University, Post-doctoral Research Project, West China Hospital, Sichuan University (2018HXBH027), and China Postdoctoral Science Foundation (2019M650248).

Appendix A. Supplementary material

Supplementary data to this article can be found online at <https://doi.org/10.1016/j.jare.2019.06.002>.

References

- [1] Schneekloth AR, Pucheault M, Tae HS, Crews CM. Targeted intracellular protein degradation induced by a small molecule: En route to chemical proteomics. *Bioorg Med Chem Lett* 2008;18(22):5904–8.
- [2] Ye H, Wu W, Liu Z, Xie C, Tang M, Li S, et al. Bioactivity-guided isolation of anti-inflammation flavonoids from the stems of *Millettia dielsiana* Harms. *Fitoterapia* 2014;95(2):154–9.
- [3] Tang H, Pei HY, Wang TJ, Chen K, Wu B, Yang QN, et al. Flavonoids and biphenylneolignans with anti-inflammatory activity from the stems of *Millettia griffithii*. *Bioorg Med Chem Lett* 2016;26(18):4417–22.
- [4] Ngamga D, Fanso Free SN, Tane P, Fomum ZT, Millaurine A, a new guanidine alkaloid from seeds of *Millettia laurentii*. *Fitoterapia* 2007;78(3):276–7.
- [5] Deyou T, Gumula I, Pang F, Gruhonjic A, Mumo M, Holleran J, et al. Rotenoids, Flavonoids, and Chalcones from the Root Bark of *Millettia usaramensis*. *J Nat Prod* 2015;78(12):2932–9.
- [6] Yenesew A, Midiwo JO, Waterman PG. Rotenoids, isoflavones and chalcones from the stem bark of *Millettia usaramensis* subspecies usaramensis. *Phytochemistry* 1998;47(2):295–300.
- [7] Rajemiarimiraho M, Banzouzi JT, Rakotonandrasana SR, Chalard P, Benoit-Vical F, Rasoanaivo LH, et al. Pyranocoumarin and triterpene from *Millettia richardiana*. *Nat Prod Commun* 2013;8(8):1099–100.
- [8] Mai HDT, Nguyen TTO, Pham VC, Litaudon M, Guéritte F, Tran DT, et al. Cytotoxic prenylated isoflavone and bipterocarpan from *Millettia pachyloba*. *Planta Med* 2010;76(15):1739–42.
- [9] Na Z, Fan QF, Song QS, Hu HB. Three new flavonoids from *Millettia pachyloba*. *Phytochem Lett* 2017;19:215–9.
- [10] Na Z, Song QS, Fan QF. New Xanthone from *Millettia pachyloba* Drake. *Rec Nat Prod* 2019. doi: <https://doi.org/10.25135/rnp.116.18.10.1020>.
- [11] Mathew R, Karantza-Wadsworth V, White E. Role of autophagy in cancer. *Nat Rev Cancer* 2007;7:961–7.
- [12] Nassour J, Radford R, Correia A, Fusté JM, Schoell B, Jauch A, et al. Autophagic cell death restricts chromosomal instability during replicative crisis. *Nature* 2019;565(7741):659–63.
- [13] Yankep E, Njamen D, Fotsing MT, Fomum ZT, Mbanya JC, Giner RM, et al. Griffonianone D, an isoflavone with anti-inflammatory activity from the root bark of *Millettia griffoniana*. *J Nat Prod* 2003;66(9):1288–90.
- [14] Derese S, Barasa L, Akala HM, Yusuf AO, Kamau E, Heydenreich M, et al. 4'-Prenyloxyderrone from the stem bark of *Millettia oblata* ssp. *teitensis* and the antiplasmodial activities of isoflavones from some *Millettia* species. *Phytochemistry* 2014;8:69–72.
- [15] Adem FA, Kuete V, Mbaveng AT, Heydenreich M, Koch A, Ndakala A, et al. Cytotoxic flavonoids from two *Lonchocarpus* species. *Nat Prod Res* 2018;16:1–9.
- [16] Ding WX, Ni HM, Gao W, Hou YF, Melan MA, Chen X, et al. Differential effects of endoplasmic reticulum stress-induced autophagy on cell survival. *J Biol Chem* 2007;282(7):4702–10.
- [17] Ding W, Ni H, Li M, Liao Y, Chen X, Stolz DB, et al. Nix is critical to two distinct phases of mitophagy, reactive oxygen species-mediated autophagy induction and parkin-ubiquitin-p62-mediated mitochondrial priming. *J Biol Chem* 2010;285(36):27879–90.
- [18] Ren Y, Benatrehina PA, Muñoz Acuña U, Yuan C, Chai HB, Ninh TN, et al. Isolation of Bioactive Rotenoids and Isoflavonoids from the Fruits of *Millettia caerulea*. *Planta Med* 2016;82(11–12):1096–104.
- [19] Wen R, Lv H, Jiang Y, Tu P. Anti-inflammatory isoflavones and isoflavanones from the roots of *Pongamia pinnata* (L.) Pierre. *Bioorg Med Chem Lett* 2018;28(6):1050–5.
- [20] Dagne E, Bekele A. C -prenylated isoflavones from *Millettia ferruginea*. *Phytochemistry* 1990;29(8):2679–82.
- [21] Rukachaisirikul V, Ritthiwigrom T, Pinsa A, Sawangchote P, Taylor WC. Xanthones from the stem bark of *Garcinia nigrolineata*. *Phytochemistry* 2003;64(6):1149–56.
- [22] Deyou T, Marco M, Heydenreich M, Pan F, Gruhonjic A, Fitzpatrick PA, et al. Isoflavones and rotenoids from the leaves of *Millettia oblata* ssp. *teitensis*. *J Nat Prod* 2017;80(7):2060–6.
- [23] Yenesew A, Midiwo JO, Waterman PG. 6-Methoxycalopogonium isoflavone a: a new isoflavone from the seed pods of *Millettia dura*. *J Nat Prod* 1997;60(8):806–7.
- [24] Dagne E, Bekele A, Waterman PG. The flavonoids of *Millettia ferruginea* subsp. *ferruginea* and subsp. *darassana* in ethiopia. *Phytochemistry* 1989;28(7):1897–900.
- [25] Yenesew A, Midiwo JO, Waterman PG. Four isoflavones from seed pods of *Millettia dura*. *Phytochemistry* 1996;41(3):951–5.
- [26] Gong T, Wang DX, Chen RY, Liu P, Yu DQ. Novel benzil and isoflavone derivatives from *Millettia dielsiana*. *Planta Med* 2009;75(3):236–42.
- [27] Dagne E, Mammo W, Sterner O. Flavonoids of *Tephrosia polyphylla*. *Phytochemistry* 1992;31(10):3662–3.
- [28] Gong T, Zhang T, Wang DX, Chen RY, Liu P, Yu DQ. Two new isoflavone glycosides from the vine stem of *Millettia dielsiana*. *J Asian Nat Prod Res* 2014;16(2):181–6.
- [29] Chuankhayan P, Hua Y, Svasti J, Sakdarat S, Sullivan PA, Ketudat Cairns JR. Purification of an isoflavonoid 7-O-beta-apiosyl-glucoside beta-glycosidase and its substrates from *Dalbergia nigrescens* Kurz. *Phytochemistry* 2005;66(16):1880–9.
- [30] Chuankhayan P, Rimlumduan T, Tantanuch W, Mothong N, Kongsaree PT, Metheenukul P, et al. Functional and structural differences between isoflavonoid beta-glycosidases from *Dalbergia* sp. *Arch Biochem Biophys* 2007;468(2):205–16.
- [31] Miyase T, Sano M, Nakai H, Muraoka M, Nakazawa M, Suzuki M, et al. Antioxidants from *Lespedeza homoloba*. (I). *Phytochemistry* 1999;52(2):303–10.
- [32] Malan E, Swinny E. Flavonoids and isoflavonoids from the heartwood of *Virgilia oroboides*. *Phytochemistry* 1990;29(10):3307–9.
- [33] Nayak M, Jung Y, Kim I. Syntheses of pterocarpenes and coumestans via regioselective cyclodehydration. *Org Biomol Chem* 2016;14(34):8074–87.

- [34] Feng ZG, Bai WJ, Pettus TR. Unified total syntheses of (-)-medicarpin, (-)-sophoracarpin A, and (±)-kushecarpin A with some structural revisions. *Angew Chem Int Ed Engl* 2015;54(6):1864–7.
- [35] Abdel-Kader MS. Phenolic constituents of *Ononis vaginalis* roots. *Planta Med* 2001;67(4):388–90.
- [36] Calter MA, Li N. Asymmetric total syntheses of (-)-variabilin and (-)-glycinol. *Org Lett* 2011;13(14):3686–9.
- [37] Kato-Noguchi H. Isolation and identification of an allelopathic substance in *Pisum sativum*. *Phytochemistry* 2003;62(7):1141–4.
- [38] Kim YS, Ryu YB, Curtis-Long MJ, Yuk HJ, Cho JK, Kim JY, et al. Flavanones and rotenoids from the roots of *Amorpha fruticosa* L. that inhibit bacterial neuraminidase. *Food Chem Toxicol* 2011;49(8):1849–56.
- [39] Fechner J, Kaufmann M, Herz C, Eisenschmidt D, Lamy E, Kroh LW, Hanschen FS. The major glucosinolate hydrolysis product in rocket (*Eruca sativa* L.), sativin, is 1,3-thiazepane-2-thione: Elucidation of structure, bioactivity, and stability compared to other rocket isothiocyanates. *Food Chem* 2018;261:57–65.
- [40] Della GM, Molinaro A, Monaco P, Previtiera L. Neolignans from *Arum italicum* [rhizomes]. *Phytochemistry* 1994;35(3):777–9.
- [41] Jerković I, Hegić G, Marijanović Z, Bubalo D. Organic extractives from *Mentha* spp. honey and the bee-stomach: methyl syringate, vomifoliol, terpenediol I, hotrienol and other compounds. *Molecules* 2010;15(4):2911–24.
- [42] Park E, Kim MC, Choi CW, Kim J, Jin HS, Lee R, et al. Effects of dihydrophaseic acid 3'-O-β-d-glucopyranoside isolated from *Lycii radidis* cortex on osteoblast differentiation. *Molecules* 2016;21(9). pii : E1260.
- [43] Alina U, Stefanie S, Philipp G, Corina I, Cristina AI, Michael L. The Impact of soy isoflavones on MCF-7 and MDA-MB-231 breast cancer cells using a global metabolomic approach. *Int J Mol Sci* 2016;17(9). pii: E1443.
- [44] Xiao JX, Huang GQ, Geng X, Qiu XW. Soy-derived isoflavones inhibit HeLa cell growth by inducing apoptosis. *Plant Foods Hum Nutr* 2011;66(2):122–8.
- [45] Huang HC, Syu KY, Lin JK. Chemical composition of *Solanum nigrum* linn extract and induction of autophagy by leaf water extract and its major flavonoids in AU565 breast cancer cells. *J Agric Food Chem* 2010;58(15):8699–708.
- [46] Kai J, Wei W, Xin J, Zhaoyang W, Zhiwei J, Guanmin M. Silibinin, a natural flavonoid, induces autophagy via ROS-dependent mitochondrial dysfunction and loss of ATP involving BNIP3 in human MCF7 breast cancer cells. *Oncol Rep* 2015;33(6):2711–8.
- [47] Peterson J, Dwyer J. Flavonoids: Dietary occurrence and biochemical activity. *Nutr Res* 1998;18(12):1995–2018.
- [48] Klionsky DJ, Cuervo AM, Seglen PO. Methods for Monitoring Autophagy from Yeast to Human. *Autophagy* 2007;3(3):181–206.